High precision ground-based photometry with 1-m class telescopes

M. Lendl

Space Research Institute, Austrian Academy of Sciences, (E-mail: monika.lendl@oeaw.ac.at)

Abstract. Recent years have seen an improvement of photometric precision with ground-based observatories routinely achieving a relative precision at the sub-mmag level. With optimized instrumentation and observing strategies, as well as ample time resources, ground-based 1m-class facilities are important players in a wide range of fields. I here summarize the main instrumental and observational strategies conductive to obtaining high-precision ground-based photometry, and review data analysis methods to account for instrumental correlated noise. Finally, I review the main applications of high-precision photometry related to the search for, and characterization of, extrasolar planets.

Key words: photometry – exoplanets – observing techniques

1. Introduction

The technique of monitoring the brightness of stars, photometry, is one of the fundamental pillars of observational astronomy. Thanks to major advances in technology (in particular the rise of CDD detectors, which have enabled digitized data processing), the attainable precision has improved by several orders of magnitude over the last few decades. While measurements at the part-per-million level remain reserved for space mission such as Kepler (Borucki et al., 2010), TESS (Ricker et al., 2014) and soon CHEOPS (Broeg et al., 2013), small ground-based observatories have shown to routinely achieve precisions at the sub-mmag level. Operating at this level of precision, small ground-based telescopes have become key players in a wide variety of fields, ranging from Solar System research to extragalactic astronomy. Ground-based photometry with 1m-class telescopes benefits from ample time resources, cost-efficient facilities and high operational flexibility.

In the following, I summarize the main aspects of instrumentation related to high-precision ground-based telescopes and detail the most common observational and data analysis strategies. I further review recent results of high-precision photometry in the framework of exoplanet research.

2. Instrumentation, observing techniques and data analysis

2.1. Optimizing instrument and setup

Most current set-ups for photometric instruments at 1-m class telescopes consist of a CCD camera paired with a set of photometric filters designed to match – as closely as possible – the requirements imposed on the system by its scientific purpose. The wavelength range often presents a prime constraint, as some observations might target specific emission or absorption lines, obtain precise measurements across different wavelength ranges, or simply maximize the overall photometric precision. To this end, back-illuminated CCDs have found widespread use as these offer improved quantum efficiencies compared to traditional front-illuminated designs. Further enhancements in terms of S/N can be reached by using deep-depletion chips, which allow for better efficiency towards the near-IR.

While improved quantum efficiency and broad filters serve to optimize the signal photon noise, detector readout noise and thermal noise (*dark current*) can remain an issue. The former may be limited by choosing optimal exposure times that both, maximize the duty cycle and limit the number of readouts necessary. The latter can be efficiently controlled by actively cooling the instrument. While temperatures below -100 C previously necessitated the use of coolants such as liquid Nitrogen, low temperatures can now be obtained through multi-stage Peltier elements.

Finally, uneven CCD sensitivity and system throughput manifest in flat field variations across the detector frame. While occasional cleaning of detector entrance window and filters can help reduce some flat field inhomogeneities, defects located at the CCD itself cannot be easily eliminated. In practice, the best way for the user to avoid these is to map their location on the CCD and optimize pointing such that no imperfections coincide with any target of interest.

2.2. Observing techniques

Any observation using relative photometry is naturally limited by the quality and number of the available reference sources. The first and most basic step for successful high-precision photometry thus consists in optimizing the pointing direction such that the field of view contains a maximum number of stable reference sources with magnitudes similar to that of the target. As the on-sky density of stars of a given magnitude decreases drastically for bright stars, the need to fit at least two objects onto the detector usually places a natural limit on the typical magnitudes accessible by any given instrument. Small telescopes here benefit from large fields of view that allow them to often outperform large facilities on bright stars.

Two approaches are commonly used (often in concert) to minimize the effects of detector sensitivity variations in high precision photometry:

– **Improved guiding:** Ideally, if the targets' location on the detector is invariant, the flat-field remains constant throughout the observations. Precise guiding is employed to approach as much as possible to this ideal case. However, many 1-m class telescopes do not possess their own guiding camera. This situation can be remedied by employing a self-guiding mechanism using the science frames to measure guiding drifts. If absolute positional information is required, this can be done matching the frames against a catalog (as done e.g. with EulerCam, Lendl et al., 2012). Alternatively, frames can also be matched directly against each other using e.g. the DONUTS algorithm (McCormac et al., 2013).

– **Widening the PSF:** The second approach to limit flat-field effects consists in artificially widening the stellar PSFs on the detector. Most commonly, this is done by slightly defocusing the telescope and thereby spreading the starlight over many pixels and averaging out sensitivity variations. An added advantage of this technique is that exposure times can be increased without saturating the detector, which in turn leads to improved duty cycles and observation efficiency. Defocusing has been used widely, and Figure 1 shows a typical PSF of a defocused observation (Southworth et al., 2009) dedicated to exoplanet science. Recently, also diffusers have been used to this end, leading to encouraging results (Stefansson et al., 2017, 2018). Limits of this technique are naturally imposed by the observed field. Well-suited to low-density star fields or bright stars, defocusing will decrease the overall precision when crowded fields, e.g. stellar clusters, are observed and defocusing leads to a high degree of blended sources.
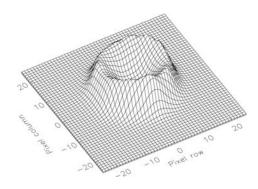

Figure 1. Example of a heavily defocused PSF by Southworth et al. (2009).

2.3. Data analysis techniques

Once photometry has been obtained and extracted, relative photometry is usu-
ally obtained by constructing a reference source by co-adding several stable
field stars and dividing the target by this reference flux. At this point, the most
prominent signatures of the Earth's atmosphere, such as variable transparency
and absorption due to changing air mass, are removed. Usually however, at this
point, a light curve is not entirely free of systematic effects. These are often
smooth trends caused by differential extinction and sky background variations,
or effects due to variable seeing or pointing jitter. As this *red noise* is usu-
ally related to external parameters, we can attempt to model its behavior and
eventually account for it when making astrophysical inferences. To do so, two
methods are currently widely used.

– **Parametric baseline models:** In this approach, one assumes that the
  red noise can be approximated by parametric functions of a set of state
  variables ($\bar{\xi}$) describing the observations. Typical state variables are time
  (t), the stellar FWHM, coordinate offsets ($\Delta x, \Delta y$), or the sky background
  (see e.g. Gillon et al., 2010, 2012). One then assumes that the observed signal
  can be modeled by an equation of the form

  $$F(t) = M(t)\,B(\bar{\xi})\,,\qquad\qquad(1)$$

  where $F(t)$ is the observed flux, $M(t)$ is the astrophysical effect and $B(\bar{\xi})$ is
  the photometric baseline function. In principle, $B(\bar{\xi})$ may take any analytic
  form deemed adequate, however, it is most commonly assumed to be rela-
  tively simple, such as combinations of low-order polynomials. As an example
  $B(\bar{\xi})$ may be a second-order polynomial in time combined with a linear drift
  in coordinate shifts:

  $$B(t, \Delta x, \Delta y) = A_0 + A_1 t + A_2 t^2 + A_3 \Delta x + A_4 \Delta y\,,\qquad(2)$$

  where A_i are coefficients. To correctly propagate errors, baseline coefficients
  are best fitted at the same time as the astrophysical model. Further, care
  should be taken at selecting the most appropriate baseline model and avoid
  over-fitting. A common approach for model selection is via the Bayesian In-
  formation Criterion (e.g. Schwarz, 1978). When several models show similar
  evidence, it is advantageous to combine results obtained from a range of
  models to avoid biasing the results (Gibson, 2014).

– **Gaussian processes:** Often correlations are too complex to be easily de-
  scribed with parametric models, or their dependence on external parameters
  does not follow a simple analytic form. In this case, Gaussian Processes offer
  a remedy to account for red noise in the data analysis while at the same time
  correctly accounting for uncertainties (see e.g. Rasmussen & Williams, 2006
  for a detailed introduction to GPs). In short, within the GP framework, a

time-series is interpreted as a multivariate Gaussian distribution around a mean function defined by the astrophysical model and having a covariance matrix C. The elements of the covariance matrix take a functional form (the *kernel*). An example of a widely used kernel is the square exponential kernel,

$$C_{i,j} = \xi \exp\left(-\frac{1}{2}\frac{(t_i - t_j)^2}{l}\right),\qquad(3)$$

where ξ denotes the maximum covariance and l is the length scale parameter. In this example, time is the only state variable included, however kernels incorporating one or several other state variables are easily devised. If desired, an additional term $\delta_{i,j}\sigma^2$ can be added to account for extra white noise. As with parametric models, the kernel parameters *"hyperparameters"* are usually fit at the same time as the parameters of the mean function. Since the introduction of GPs to high precision photometry (Gibson et al., 2012), several open-source software packages (Aigrain et al., 2016; Foreman-Mackey et al., 2017) have become available simplifying the use of GPs in the framework of light curve analysis.

3. High-precision photometry for exoplanet science

Transiting exoplanets have been one of the key fields pushing ground-based photometric observations to their optimum: for the detection of transiting sub-Joivan planets, relative precisions at the sub-mmag level have to be obtained throughout several hours. Furthermore, photometric observations open up a range of charcterization avenues. I will briefly outline a set of projects and results related to exoplanets that have been obtained with 1-m class telescopes.

3.1. Transit searches and follow-up

Until the advent of the TESS space mission (Ricker et al., 2014), ground based surveys were the only means of discovering transiting planets across the entire sky. While monitoring mostly relied on very small aperture facilities (e.g. Bakos et al., 2004; Pollacco et al., 2006), 1-m-class facilities have been instrumental in the follow-up efforts, eliminating false positives such as blended eclipsing binaries, and obtaining high-precision transit light curves. Figure 2 shows an example of a follow-up transit light curve of the hot Jupiter WASP-164b observed with the 1.2m Euler telescope. Some surveys have been making use of 1-m-class instrumentation (e.g. OGLE (Konacki et al., 2003), NGTS (Wheatley et al., 2018) and TRAPPIST-UCDTS/SPECULOOS (Gillon et al., 2016; Delrez et al., 2018a)) to search for the signatures of transiting planets. In these cases, the choice for larger instruments has mostly been driven by needs of observing faint sources (see e.g. the discovery of a planetary system around an ultra-cool dwarf, Gillon et al. 2016), or the need for high photometric precision (see e.g. the detection of a sub-Neptune, West et al. 2018).
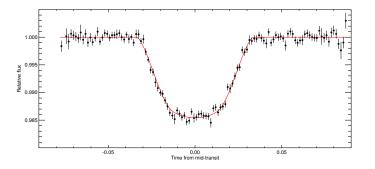
Figure 2. Follow-up photometry for the hot Jupiter WASP-164 obtained with Euler-Cam at the 1.2m Euler telescope, Lendl et al. (2019).

3.2. Atmospheric characterization: occultations and transmission spectra

Going beyond the mere detection of exoplanets, 1-m class ground-based facilities have also provided ample opportunities to study these planets in detail. For hot Jupiters (close-in gas giants), thermal emission from the planetary dayside produces occultation depths of several hundreds of ppm in the red optical or near-IR (I or z' band). By combining several individual occultation light curves, 1-m class facilities have secured a number of detections (Abe et al., 2013; Lendl et al., 2013; Mancini et al., 2013; Delrez et al., 2016, 2018b). The example of the hot Jupiter WASP-103b (Delrez et al., 2018b), a detection for which 13 individual light curves were combined, is shown in Figure 3.

Similarly, precise measurements of transit light curves at different wavelengths allow to obtain a planetary transmission spectrum at low resolution. While the most prominent features of Na and K (Seager & Sasselov, 2000; Charbonneau et al., 2002) are too narrow-band to be accessible with small facilities, broad spectral features, such as slopes due to high-altitude hazes can be detected (Pont et al., 2008). A wide range of facilities and observing programs (e.g. de Mooij et al., 2012; Mancini et al., 2013; Mallonn et al., 2015; Southworth et al., 2017) have been dedicated to this science case. As an example, the detection of increased atmospheric absorption towards the blue (as expected from high-altitude hazes), in the hot Jupiter WASP-36b is shown in Figure 4. Since stellar spots (occulted or unoculted during transit) can bias the observed transit depth, this technique is most ideally pursued with simultaneous multi-band observations.
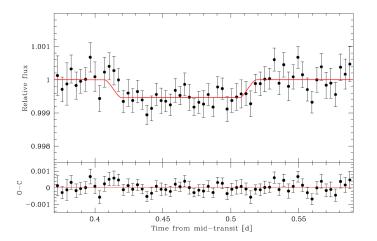
Figure 3. Occultation light curve of the hot Jupiter WASP-103b (Delrez et al., 2018b) using EulerCam and TRAPPIST.
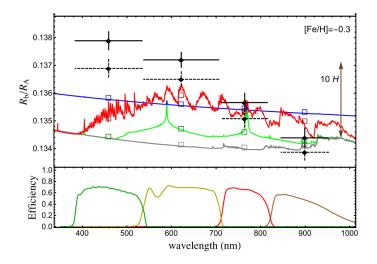

Figure 4. Low-resolution transmission spectrum of WASP-36 by Mancini et al. (2016) using the MPG 2.2m telescope.

3.3. Transit timing variations

While in single-planet systems, transits are expected to occur in equally-spaced intervals, the observed transit periods can vary in multi-planet systems, owing to the dynamical interactions between the host and its several planets. If detected, these *transit timing variations (TTVs)* (Agol et al., 2005; Holman & Murray, 2005) can reveal additional planets and serve to measure planet masses. For extremely close-in planets, TTVs can even occur due to tidal interactions between the planet and the host: planets are losing angular momentum and slowly spiraling into inwards. Measuring the decay rate of the planetary orbit can thus reveal the dissipation of tidal energy in the host star, constraining the tidal quality parameter Q'_* (see e.g. Collier Cameron & Jardine, 2018, and references therein). A range of surveys have targeted hot Jupiters with 1m-class facilities, searching for TTVs (e.g. Holman et al., 2006; Lendl et al., 2010; Maciejewski et al., 2010). While TTVs can be substantial for planets in multiplanet systems (e.g. Holman et al., 2010), tentative evidence for a period decay has only been found in one hot Jupiter to date (Maciejewski et al., 2018). The same technique can be used to determine the nature of planet candidates identified by the Kepler satellite (von Essen et al., 2018), in cases where the radial-velocity method cannot be used (e.g. faint objects).
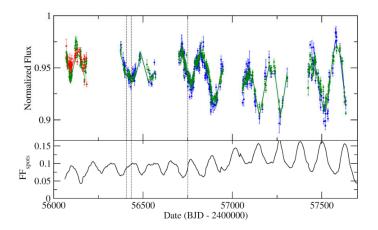

Figure 5. The long-term variability (top) and spot filling factors (bottom) of the planet host star GJ 1214 by Mallonn et al. (2018).

3.4. Stellar hosts

Next to the planets themselves, information on the activity and rotation of stellar hosts can be gathered with high-precision photometry. This is either done

through long-term monitoring (e.g. Mallonn et al., 2018, see Fig, 5), capturing the stellar variability induced as star spots move in- and out-of view. In transit light curves observed at very high precision, short-term brightenings have been observed (Tregloan-Reed et al., 2013; Juvan et al., 2018). These can be attributed to the planet crossing over a star spot, and consequently blocking light from a less emissive stellar region. As similar short-term variations can easily be due to correlated noise rather than a physical effect, simultaneous observations from several facilities have shown to help to distinguish real star spot crossings from instrumental systematics (e.g. Lendl et al., 2013; Mancini et al., 2017; Juvan et al., 2018). When observed in several subsequent transits, spot crossings can reveal the stellar rotation rate and constrain the planetary orbital obliquity.

References

Abe, L., Gonçalves, I., Agabi, A., et al., The secondary eclipses of WASP-19b as seen by the ASTEP 400 telescope from Antarctica. 2013, *Astron. Astrophys.*, **553**, A49, DOI: 10.1051/0004-6361/201220351

Agol, E., Steffen, J., Sari, R., & Clarkson, W., On detecting terrestrial planets with timing of giant planet transits. 2005, *Mon. Not. R. Astron. Soc.*, **359**, 567, DOI: 10.1111/j.1365-2966.2005.08922.x

Aigrain, S., Parviainen, H., & Pope, B. J. S., K2SC: flexible systematics correction and detrending of K2 light curves using Gaussian process regression. 2016, *Mon. Not. R. Astron. Soc.*, **459**, 2408, DOI: 10.1093/mnras/stw706

Bakos, G., Noyes, R. W., Kovács, G., et al., Wide-Field Millimagnitude Photometry with the HAT: A Tool for Extrasolar Planet Detection. 2004, *Publ. Astron. Soc. Pac.*, **116**, 266, DOI: 10.1086/382735

Borucki, W. J., Koch, D., Basri, G., et al., Kepler Planet-Detection Mission: Introduction and First Results. 2010, *Science*, **327**, 977, DOI: 10.1126/science.1185402

Broeg, C., Fortier, A., Ehrenreich, D., et al., CHEOPS: A transit photometry mission for ESA's small mission programme. 2013, in European Physical Journal Web of Conferences, Vol. **47**, *European Physical Journal Web of Conferences*, 03005

Charbonneau, D., Brown, T. M., Noyes, R. W., & Gilliland, R. L., Detection of an Extrasolar Planet Atmosphere. 2002, *Astrophys. J.*, **568**, 377, DOI: 10.1086/338770

Collier Cameron, A. & Jardine, M., Hierarchical Bayesian calibration of tidal orbit decay rates among hot Jupiters. 2018, *ArXiv e-prints* [[arXiv]1801.10561]

de Mooij, E. J. W., Brogi, M., de Kok, R. J., et al., Optical to near-infrared transit observations of super-Earth GJ 1214b: water-world or mini-Neptune? 2012, *Astron. Astrophys.*, **538**, A46, DOI: 10.1051/0004-6361/201117205

Delrez, L., Gillon, M., Queloz, D., et al., SPECULOOS: a network of robotic telescopes to hunt for terrestrial planets around the nearest ultracool dwarfs. 2018a, in Society of Photo-Optical Instrumentation Engineers (SPIE) Conference Series, Vol. **10700**, *Ground-based and Airborne Telescopes VII*, 107001I

Delrez, L., Madhusudhan, N., Lendl, M., et al., High-precision multiwavelength eclipse photometry of the ultra-hot gas giant exoplanet WASP-103 b. 2018b, *Mon. Not. R. Astron. Soc.*, **474**, 2334, DOI: 10.1093/mnras/stx2896

Delrez, L., Santerne, A., Almenara, J.-M., et al., WASP-121 b: a hot Jupiter close to tidal disruption transiting an active F star. 2016, *Mon. Not. R. Astron. Soc.*, **458**, 4025, DOI: 10.1093/mnras/stw522

Foreman-Mackey, D., Agol, E., Ambikasaran, S., & Angus, R., Fast and Scalable Gaussian Process Modeling with Applications to Astronomical Time Series. 2017, *Astron. J.*, **154**, 220, DOI: 10.3847/1538-3881/aa9332

Gibson, N. P., Reliable inference of exoplanet light-curve parameters using deterministic and stochastic systematics models. 2014, *Mon. Not. R. Astron. Soc.*, **445**, 3401, DOI: 10.1093/mnras/stu1975

Gibson, N. P., Aigrain, S., Roberts, S., et al., A Gaussian process framework for modelling instrumental systematics: application to transmission spectroscopy. 2012, *Mon. Not. R. Astron. Soc.*, **419**, 2683, DOI: 10.1111/j.1365-2966.2011.19915.x

Gillon, M., Jehin, E., Lederer, S. M., et al., Temperate Earth-sized planets transiting a nearby ultracool dwarf star. 2016, *Nature*, **533**, 221, DOI: 10.1038/nature17448

Gillon, M., Lanotte, A. A., Barman, T., et al., The thermal emission of the young and massive planet CoRoT-2b at 4.5 and 8 μm. 2010, *Astron. Astrophys.*, **511**, A3, DOI: 10.1051/0004-6361/200913507

Gillon, M., Triaud, A. H. M. J., Fortney, J. J., et al., The TRAPPIST survey of southern transiting planets. I. Thirty eclipses of the ultra-short period planet WASP-43 b. 2012, *Astron. Astrophys.*, **542**, A4, DOI: 10.1051/0004-6361/201218817

Holman, M. J., Fabrycky, D. C., Ragozzine, D., et al., Kepler-9: A System of Multiple Planets Transiting a Sun-Like Star, Confirmed by Timing Variations. 2010, *Science*, **330**, 51, DOI: 10.1126/science.1195778

Holman, M. J. & Murray, N. W., The Use of Transit Timing to Detect Terrestrial-Mass Extrasolar Planets. 2005, *Science*, **307**, 1288, DOI: 10.1126/science.1107822

Holman, M. J., Winn, J. N., Latham, D. W., et al., The Transit Light Curve Project. I. Four Consecutive Transits of the Exoplanet XO-1b. 2006, *Astrophys. J.*, **652**, 1715, DOI: 10.1086/508155

Juvan, I. G., Lendl, M., Cubillos, P. E., et al., PyTranSpot: A tool for multiband light curve modeling of planetary transits and stellar spots. 2018, *Astron. Astrophys.*, **610**, A15, DOI: 10.1051/0004-6361/201731345

Konacki, M., Torres, G., Jha, S., & Sasselov, D. D., An extrasolar planet that transits the disk of its parent star. 2003, *Nature*, **421**, 507, DOI: 10.1038/nature01379

Lendl, M., Afonso, C., Koppenhoefer, J., et al., New parameters and transit timing studies for OGLE2-TR-L9 b. 2010, *Astron. Astrophys.*, **522**, A29, DOI: 10.1051/0004-6361/201014940

Lendl, M., Anderson, D. R., Bonfanti, A., et al., WASP-147b, 160Bb, 164b, and 165b: two hot Saturns and two Jupiters, including two planets with metal-rich hosts. 2019, *Mon. Not. R. Astron. Soc.*, **482**, 301, DOI: 10.1093/mnras/sty2667

Lendl, M., Anderson, D. R., Collier-Cameron, A., et al., WASP-42 b and WASP-49 b: two new transiting sub-Jupiters. 2012, *Astron. Astrophys.*, **544**, A72, DOI: 10.1051/0004-6361/201219585

Lendl, M., Gillon, M., Queloz, D., et al., A photometric study of the hot exoplanet WASP-19b. 2013, *Astron. Astrophys.*, **552**, A2, DOI: 10.1051/0004-6361/201220924

Maciejewski, G., Dimitrov, D., Neuhäuser, R., et al., Transit timing variation in exoplanet WASP-3b. 2010, *Mon. Not. R. Astron. Soc.*, **407**, 2625, DOI: 10.1111/j.1365-2966.2010.17099.x

Maciejewski, G., Fernández, M., Aceituno, F., et al., Planet-star interactions with precise transit timing. I. The refined orbital decay rate for WASP-12 b and initial constraints for HAT-P-23 b, KELT-1 b, KELT-16 b, WASP-33 b, and WASP-103 b. 2018, *arXiv e-prints* [[arXiv]1812.02438]

Mallonn, M., Herrero, E., Juvan, I. G., et al., GJ 1214: Rotation period, starspots, and uncertainty on the optical slope of the transmission spectrum. 2018, *Astron. Astrophys.*, **614**, A35, DOI: 10.1051/0004-6361/201732300

Mallonn, M., Nascimbeni, V., Weingrill, J., et al., Broad-band spectrophotometry of the hot Jupiter HAT-P-12b from the near-UV to the near-IR. 2015, *Astron. Astrophys.*, **583**, A138, DOI: 10.1051/0004-6361/201425395

Mancini, L., Ciceri, S., Chen, G., et al., Physical properties, transmission and emission spectra of the WASP-19 planetary system from multi-colour photometry. 2013, *Mon. Not. R. Astron. Soc.* [[arXiv]1306.6384], DOI: 10.1093/mnras/stt1394

Mancini, L., Kemmer, J., Southworth, J., et al., An optical transmission spectrum of the giant planet WASP-36 b. 2016, *Mon. Not. R. Astron. Soc.*, **459**, 1393, DOI: 10.1093/mnras/stw659

Mancini, L., Southworth, J., Raia, G., et al., Orbital alignment and star-spot properties in the WASP-52 planetary system. 2017, *Mon. Not. R. Astron. Soc.*, **465**, 843, DOI: 10.1093/mnras/stw1987

McCormac, J., Pollacco, D., Skillen, I., et al., DONUTS: A Science Frame Autoguiding Algorithm with Sub-Pixel Precision, Capable of Guiding on Defocused Stars. 2013, *Publ. Astron. Soc. Pac.*, **125**, 548, DOI: 10.1086/670940

Pollacco, D. L., Skillen, I., Collier Cameron, A., et al., The WASP Project and the SuperWASP Cameras. 2006, *Publ. Astron. Soc. Pac.*, **118**, 1407, DOI: 10.1086/508556

Pont, F., Knutson, H., Gilliland, R. L., Moutou, C., & Charbonneau, D., Detection of atmospheric haze on an extrasolar planet: the 0.55-1.05 μm transmission spectrum of HD 189733b with the HubbleSpaceTelescope. 2008, *Mon. Not. R. Astron. Soc.*, **385**, 109, DOI: 10.1111/j.1365-2966.2008.12852.x

Rasmussen, S. & Williams, C. 2006, *Gaussian Processes for Machine Learning* (The MIT Press)

Ricker, G. R., Winn, J. N., Vanderspek, R., et al., Transiting Exoplanet Survey Satellite (TESS). 2014, in Proc. SPIE, Vol. **9143**, *Space Telescopes and Instrumentation 2014: Optical, Infrared, and Millimeter Wave*, 914320

Schwarz, Estimating the Dimension of a Model. 1978, *Annals of Statistics*, **6**, 461

Seager, S. & Sasselov, D. D., Theoretical Transmission Spectra during Extrasolar Giant Planet Transits. 2000, *Astrophys. J.*, **537**, 916, DOI: 10.1086/309088

Southworth, J., Hinse, T. C., Jørgensen, U. G., et al., High-precision photometry by telescope defocusing - I. The transiting planetary system WASP-5. 2009, *Mon. Not. R. Astron. Soc.*, **396**, 1023, DOI: 10.1111/j.1365-2966.2009.14767.x

Southworth, J., Mancini, L., Madhusudhan, N., et al., Detection of the Atmosphere of the 1.6 M Exoplanet GJ 1132 b. 2017, *Astron. J.*, **153**, 191, DOI: 10.3847/1538-3881/aa6477

Stefansson, G., Li, Y., Mahadevan, S., et al., Diffuser-assisted Photometric Follow-up Observations of the Neptune-sized Planets K2-28b and K2-100b. 2018, *Astron. J.*, **156**, 266, DOI: 10.3847/1538-3881/aae6ca

Stefansson, G., Mahadevan, S., Hebb, L., et al., Toward Space-like Photometric Precision from the Ground with Beam-shaping Diffusers. 2017, *Astrophys. J.*, **848**, 9, DOI: 10.3847/1538-4357/aa88aa

Tregloan-Reed, J., Southworth, J., & Tappert, C., Transits and starspots in the WASP-19 planetary system. 2013, *Mon. Not. R. Astron. Soc.*, **428**, 3671, DOI: 10.1093/mnras/sts306

von Essen, C., Ofir, A., Dreizler, S., et al., Kepler Object of Interest Network. I. First results combining ground- and space-based observations of Kepler systems with transit timing variations. 2018, *Astron. Astrophys.*, **615**, A79, DOI: 10.1051/0004-6361/201732483

West, R. G., Gillen, E., Bayliss, D., et al., NGTS-4b: A sub-Neptune Transiting in the Desert. 2018, *ArXiv e-prints* [[arXiv]1809.00678]

Wheatley, P. J., West, R. G., Goad, M. R., et al., The Next Generation Transit Survey (NGTS). 2018, *Mon. Not. R. Astron. Soc.*, **475**, 4476, DOI: 10.1093/mnras/stx2836